# THE SOUND GENERATED BY A TWO-DIMENSIONAL SHEAR LAYER: THE FAR FIELD DIRECTIVITY FROM COMPUTATIONS AND ACOUSTIC ANALOGIES

Tim Colonius*
Sanjiva K. Lele†
Parviz Moin‡
Department of Mechanical Engineering
Stanford University
Stanford CA 94305

## ABSTRACT

The sound generated by vortex pairing in a two-dimensional mixing layer is studied by direct numerical simulation of the Navier-Stokes equations (DNS) for the layer and a portion of its acoustic field, and by solving Lilley's equation (with source terms determined from the DNS) for the entire acoustic field. Predictions for the acoustic field based on Lilley's equation are in good agreement with the DNS results. The radiated acoustic field at the pairing frequencies is highly directive and cannot be produced by point quadrupole sources. Instead, it is of the superdirective character considered by Crighton and Huerre (1990, *J. Fluid Mech.*, **220**), where the magnitude of the pressure varies like the exponential of the cosine of the angle between the observation point and the downstream axis. By making modifications to this basic directivity, we account, in part, for shear in the mean velocity and the convection of the acoustic waves by the different freestream velocities on either side of the layer, and obtain a good overall agreement between the theory and the computations.

## INTRODUCTION

The sound generated by a two-dimensional compressible mixing layer is investigated using Direct Numerical Simulation (DNS) of the Navier-Stokes equations and by the solution of acoustic analogy equations. The DNS includes a portion of the acoustic field and can be compared with the acoustic field predicted by the acoustic analogy. In Colonius *et al.*(1995) we presented predictions for the sound generated by the pairing of vortices in a mixing layer from the DNS and solution of Lilley's acoustic analogy. In particular, we found that the form of the source term proposed by Goldstein (1984) gives good agreement with the DNS.

In this paper we are concerned primarily with understanding the far field directivity in terms of the simple model for superdirective sources proposed by Crighton and Huerre (1990) (hereafter referred to as CH).

*Present address: Division of Engineering and Applied Science, California Institute of Technology, Pasadena, CA 91125
†also with the Department of Aeronautics and Astronautics
‡also with the NASA-Ames Research Center

## METHODOLOGY

We summarize the methodology of the DNS and solution of the acoustic analogy – the reader is referred to Colonius (1994b) for more details. The 2D unsteady compressible Navier-Stokes equations plus conservations of mass and energy are solved numerically for the mixing layer depicted in Figure 1. The Mach numbers of the high and low speed streams are $M_1 = 0.5$ and $M_2 = 0.25$, respectively, and the temperature of the two streams is equal. Our numerical scheme for sound generation problems has been validated it on a number of model problems; see Colonius *et al.*(1993a, 1994a,b) and Mitchell *et al.*(1995a,b). In what follows all the streamwise and normal velocities $u_1$, and $u_2$ are normalized by the speed of sound far from the mixing region, $a_\infty$. Lengths $x_1$ and $x_2$ are normalized by the vorticity thickness of the layer at $x_1 = 0$. The density, $\rho$ is normalized by its value far from the mixing region, $\rho_\infty$, and the pressure, $p$, is normalized by $\rho_\infty a_\infty^2$. Frequencies (see below) are made nondimensional by multiplying by the vorticity thickness and dividing by the $a_\infty$, and wavenumbers are multiplied by the vorticity thickness.

A Cartesian grid of 2300 by 847 grid points in the $x_1$ and $x_2$ directions, respectively, is used. The grid in $x_1$ is uniform with spacing $\Delta x_1 = 0.15$ in the "physical" domain, up to $x_1 = 285$. A uniform grid spacing of $\Delta x_2 = 0.15$ is used in a region near $x_2 = 0$. The grid transitions to a uniform but coarser spacing of $\Delta x_2 = 0.80$ for large $\pm x_2$. The time step, $\Delta t$, was 0.0567. Nonreflecting boundary conditions are used at the inflow and normal boundaries, and a sponge outflow (Colonius *et al.*, 1993a) is used at the downstream computational boundary. The layer is forced at its subharmonics $f/2$, $f/4$, and $f/8$ with eigenfunctions from linear stability analysis. The phase speed of the waves, $M_c = \frac{\omega}{k_r}$, is about 0.4 for all the frequencies. The layer rolls up and pairs at stationary positions in space, and becomes very nearly periodic in time. This has the important consequence of causing the acoustic sources to be stationary, as it is in the experiments of Laufer and Yen (1983) and others.

We use a numerical method to solve an acoustic analogy for the entire acoustic field, given source terms computed from the DNS. Our starting point is the acoustic

analogy proposed by Lilley (1974), which is a generalization of Lighthill's equation for flows with mean shear:

$$D_t\left(D_t^2\Pi - (a^2\Pi_{,j})_{,j}\right) + 2u_{k,j}(a^2\Pi_{,j})_{,k} = -2u_{i,j}u_{j,k}u_{k,i}, \quad (1)$$

where $D_t$ is the convective derivative, $\frac{\partial}{\partial t} + u_k\frac{\partial}{\partial x_k}$, $\Pi$ is the logarithmic pressure defined by $\Pi = \frac{1}{\gamma}\ln p$, and we have used the shorthand that the subscript after the comma refers to differentiation with respect to that coordinate direction. Equation (1) is an exact consequence of the basic conservation principles but is a single nonlinear equations in 4 variables and therefore cannot be solved uniquely. Often the flow is well approximated by a steady parallel transversely sheared flow (i.e one for which $u_2 = 0$ and $u_1$ is only a function of $x_2$, which we denote $U(x_2)$, $\Pi$ and $\rho$ are constants) plus fluctuations (Goldstein, 1984), which we denote with a prime. Using this decomposition in (1) gives:

$$\bar{D}_t\left(\bar{D}_t^2\Pi' - \Pi'_{,jj}\right) + 2U_{,2}\Pi'_{,12} = \Gamma(x_1,x_2,t) = \bar{D}_t(u_i'u_j')_{,ij} - 2U_{,2}(u_2'u_j')_{,1j}, \quad (2)$$

plus a number of other terms, which have been shown (Colonius *et al.*, 1995) to produce negligible acoustic fields compared to those of the terms retained, and where $\bar{D}_t = \frac{\partial}{\partial t} + U(x_2)\frac{\partial}{\partial x_1}$. Equation (2) is identical to the one derived by Goldstein (1984).

Equation (2) is solved by taking the Discrete Fourier Transform in time and the (continuous) Fourier transform in the $x_1$ direction. The resulting 2nd order ODE (in $x_2$) is solved using finite differences. The Fourier transform in $x_1$ is evaluated using numerical quadrature. The solution method and its validation are discussed in detail by Colonius (1994b). The DFT of the source term $\Gamma$ must be performed with care because, although the mixing layer becomes very nearly periodic in time under the influence of the inlet forcing, there are still some low frequency components to the signal which cannot be represented in a reasonable run time. If the standard DFT of the aperiodic signal is taken, the unresolved low frequency components leak into the resolvable low frequencies (i.e. the pairing frequencies) and although these errors are small compared to the overall magnitude of the source, they lead to grossly inaccurate predictions in the acoustic field. In a previous paper (Colonius *et al.*, 1995) we discussed a DFT method which eliminates this spurious leakage at low frequencies and allows an accurate prediction of the acoustic field.

The source term $\Gamma$ can be written in other forms, by carrying the differentiations with respect to $x_i$ through the convective derivative $\bar{D}_t$ in the first term. In particular:

$$\Gamma(x_1,x_2,t) = -2u_{i,j}u_{j,k}u_{k,i} + u_k'(a^2\Pi'_{,j})_{,jk} - 2u'_{j,k}(a^2\Pi'_{,k})_{,j} \quad (3)$$

plus a number of additional terms which again were shown (Colonius *et al.*, 1995) to produce negligible acoustic fields. In this form the original Lilley source term reappears, along with additional terms which are similar to terms on the left-hand-side of Equation (2) but which contain the fluctuating velocity $u'$ rather than the parallel flow velocity $U(x_2)$. These terms are associated with scattering and refraction of the acoustic waves by fluctuations in the flow, and by the part of the mean field which is not represented by $U(x_2)$ (since the real mean field spreads). The first term is proportional to the dilatation (which is quite small at the low Mach numbers here) and is thus much smaller in physical space than the second. However, it causes an acoustic field comparable with the acoustic field from the DNS, while the second term, while much larger in physical space, primarily acts to redistribute the directivity from term 1 to a more omnidirection directivity, consistent with its being associated with scattering (Colonius *et al.*, 1995).

## RESULTS

For a more complete discussion of the results from the DNS than space allows here, the reader is referred to Colonius *et al.*(1995) where, in particular, it was shown that the results from the DNS are in good agreement with solutions of Lilley's equations with the source terms of Equations (2) and (3). The instantaneous vorticity field at $t = 68/f$ is plotted in Figure 2 and plainly shows the roll up and two subsequent pairings of the layer. The instability waves saturation locations have been determined to be $x_1 \approx 50$, 75, and 175 for the $f$, $f/2$ and $f/4$, respectively (Colonius, 1994b).

The acoustic pressure in the far field for both $f/2$ and $f/4$ is plotted versus the angle between the observation point at a distance $r$ from the source and the positive $x_1$ axis in Figure 3. The directivity is found using both $\Gamma$ from Equation (2) (hereafter referred to as the "full source") and the first term only of (3) (hereafter referred to as "Lilley's source.") The pressure has been further normalized by $\sqrt{r}$ which is the spatial decay rate for the two dimensional waves.

The directivity is complicated, but overall is strongly peaked for angles $\theta < \pm 90°$, attaining a global maximum near $\theta = -30°$. Unlike the directivity from a jet, which is symmetric about $\theta = 0$, the directivity is weaker for $\theta > 0$. The maximum directivity occurs at a cusp. The occurrence of such cusps has been discussed by Colonius (1994b) – the asymmetry of the mean velocity causes certain spatial harmonic components of the source to radiate to one side of the layer only, i.e. solutions to the wave equation for particular values of $k$ and $\omega$ are oscillatory on one side of the layer and damped on the other. For $M_1 = 0.5$ and $M_2 = 0.25$ these angles are exactly $-30°$ and $117°$ in the low and high speed streams respectively, corresponding to the two locations where cusps can be seen in Figure 3.

The directivity is also highly oscillatory – especially when the full source is used. Indeed it appears from Figure 3 that the effect of the second two terms of Equation (3) is primarily to redistribute the acoustic waves to a more

omnidirectional distribution. The greater number and amplitude of the oscillations for the full source could be the result of "interference" between the basic directivity of the sound generated by the vortex pairings, and subsequent modifications to the waves due to scattering and refraction. In fact, the overall directivity qualitatively resembles the directivity for waves which are scattered by a single vortex, see for example Figure 5 of Colonius *et al.* (1994a). It is surprising that given the relatively low Mach number of the present layer that scattering apparently plays such a large roll, and this effect is not usually observed in experiments with jets.

The overall directivity has a form very unlike that which can be produced by point (compact) sources, either stationary or convecting, in the mixing layer. The directivity produced by convecting point sources in jets has been computed, for low frequency, by Goldstein (1975,1976) and others using Equation (2) with:

$$u_i' u_j' = A_{ij} \exp(2\pi i \omega t) \delta(x_1 - Ct) \delta(x_2), \qquad (4)$$

where $A_{ij}$ is a tensor of constants, and $C$ is a constant convection velocity. Specifically, Goldstein (1975,1976) has shown that for convecting sources, Doppler factors, $(1 - C\cos\theta)^{-n}$ with $n$ as high as 5, can multiply the directivity and thus produce a highly directive acoustic field, in accord with experiments. To investigate such sources in the present flow, we use our numerical scheme for solving Lilley's equation. We set $C = 0$ because the sources are stationary for a particular frequency in our time-periodic flow. In order to solve for the point source numerically, we must replace the delta functions in (4) with sources of finite support. We choose the distribution:

$$T_{ij} = A_{ij} \exp(2\pi i \omega t) e^{-\pi(x_1/\epsilon_1)^2} e^{-\pi(x_2/\epsilon_2)^2} / (\epsilon_1 \epsilon_2), \qquad (5)$$

In the limit as $\epsilon_1$ and $\epsilon_2$ both go to zero the distribution (5) approaches (4). By experimentation, we determine that for frequencies $f/2$ and $f/4$, a source with $\epsilon_1 = \epsilon_2 = 0.1$ appears to be sufficiently small such that each of $A_{11}$, $A_{22}$ and $A_{12}$ can be considered a point source. Figure 4 shows that the resulting directivity patterns for the point quadrupole $A_{11}$, $A_{22}$ and $A_{12}$ with a frequency $f/2$ in the present mixing layer. The pressure is normalized in each case by the corresponding strength of the source. The mean velocity and shear have a dramatic effect on the directivity, compared to the directivity of the above sources in a quiescent media which would be $\cos^2\theta$, $\sin^2\theta$, and $\cos\theta\sin\theta$ for $A_{11}$, $A_{22}$ and $A_{12}$, respectively. The mean flow causes the amplitude of the waves to be increased for waves propagating upstream (i.e. angles greater than $90^\circ$) and decreased for waves propagating downstream. Note that this is the Doppler effect, but for a stationary source in a moving flow (as opposed to a convecting source relative to a stationary observer in a flow). For a stationary source the frequency of the source and observer are the same, but the waves propagating upstream have shorter wavelength and greater magnitude. This is opposite to the desired trend shown in Figure 3 and there is clearly no possibility of constructing the observed directivity from any linear combination of the point sources.

We have also solved Lilley's equation with the source in (5), but with varying values of $\epsilon_1$ and $\epsilon_2$, and thus have considered certain effects of source non-compactness. As $\epsilon_1$ and/or $\epsilon_2$ are increased from 0.1, we find that while there is a general trend towards attenuation of the directivity in the upstream direction, this effect is not of sufficient magnitude to explain the observed directivity, and additional angles of extinction occur in the directivity which are not observed in the computations. At very large values of $\epsilon_1$ and/or $\epsilon_2$ (5) gives an acoustic field which is beamed to $\pm 90^\circ$.

Clearly an alternative explanation for the directivity must be found. One possibility is that the source is of the so-called "superdirective" type, as considered by CH. The full source $\Gamma$ computed from the DNS is plotted for $f/2$ and $f/4$ at $x_2 = 0$ in Figure 5 – the source apparently has the form of a modulated envelope function whose overall width is quite large (even compared to the acoustic wavelength), we might then expect a highly directive field from such a non-compact source. Unlike the point source considered above, the Fourier transform (in $x_1$) of the modulated source will obtain a maximum at the value of $k$ corresponding the the wavenumber of the modulation, $k_0 = -\frac{\omega}{M_c}$, which at subsonic Mach numbers is well outside the range of wavenumbers which can radiate sound to the far field, which for the present flow is given by $-\omega/(1 + M_2) < k < \omega/(1 - M_1)$. For large $|k - k_0|$ the Fourier transform of the envelope function will have decayed significantly, and the wider the envelope function is (in $x_1$), the greater the rate of decay in the range of radiating wavenumbers.

In CH, a stationary acoustic media consisting of the half infinite plane ($x_2 > 0$), and with a pressure disturbance at $x_2 = 0$ having the form of a modulated traveling wave in $x_1$, i.e. $p(x_1, 0, t) = A(x) \exp(2\pi i k_0 x) \exp(i2\pi\omega t)$, where $A(x)$ is the envelope function. Then considering the acoustic field which results at large distances from the wave packet, they determine that that the directivity is of the form:

$$p \sim \sin\theta e^{aM_c \cos\theta}, \qquad (6)$$

for $A(x)$ whose Fourier transform decays exponentially fast for large $k$, where $a$ is a constant related to the overall width of the envelope function compared to the acoustic wavelength, and $M_c$ is the phase speed of the pressure disturbance at $x_2 = 0$, i.e. $M_c = \omega/k_0$.

The pressure from the DNS is plotted in Figure 6, and is similar in form to the source, $\Gamma$. The Fourier transform of the pressure is plotted as a function of $k/\omega$ for $f/2$ and $f/4$ in Figure 7, and except for a spike in the transform near $k = 0$, the transform is decaying rapidly in the acoustic range, $-0.8 < k/\omega < 2$. The shape of the envelope function is very much more complicated than those considered by CH, and consequently decay of the transform for large $|k - k_0|$ is also complicated. Roughly

speaking, however, the decay is exponential except very near $k = 0$.

Thus we expect the directivity to have a form similar to (6). In Figure 8 and Figure 9 we replot the directivity predicted for the full source term and the Lilley source, respectively. Also plotted is the directivity given by (6). $M_c$ is set to 0.4, and the constant $a$ has been adjusted in each case to attempt to match (6) to the computed directivity – the particular values of $a$ are given in the figure caption. The overall level of the directivity is also adjusted to give the best agreement with the computations. While the quantitative agreement between the computed directivity and (6) is not very good, the overall trend is basically correct with maximum directivity at shallow angles to the mixing layer and a rapid decay for large angles. Note that constant $a$ is smaller than the value of 20 predicted by CH, which in turn is smaller than the value of 45 which CH infer from the experimental measurements of Laufer and Yen for a round jet.

We now modify the model superdirectivity given by CH, to take account of some of the differences between the current flow and the model – modification of the directivity due to (1) shear in the near field, and (2) finite (and unequal) convection velocities on either side of the layer. Accounting for the convection velocities, the exponential term arising from the Fourier transform of the pressure on $x_2 = 0$ becomes:

$$\exp\left(-2\pi|k_{sp} - k_0|\right)/\epsilon, \tag{7}$$

where $k_{sp}$ is the stationary point for the mixing layer which was derived in (Colonius, 1994b):

$$k_{sp} = \begin{cases} \frac{\omega}{1-M_1^2}\left(M_1 - \frac{\cos\theta}{\sqrt{1-M_1^2\sin^2\theta}}\right), & 0 < \theta < \pi \\ \frac{\omega}{1-M_2^2}\left(M_2 - \frac{\cos\theta}{\sqrt{1-M_2^2\sin^2\theta}}\right), & -\pi < \theta < 0 \end{cases} \tag{8}$$

Note that when $M_1 = M_2 = 0$, (8) reduces to the value used by CH, $k_{sp} = -\omega\cos\theta$.

We determine the constant $\epsilon$ by forcing the exponential term (7) to pass through the Fourier transform of the pressure at $x_2 = 0$, again ignoring the spike near $k = 0$. These curves are shown in Figure 7 along with the Fourier transform of the pressure at $x_2 = 0$. The exponential function captures the overall trend of the transformed pressure with $\epsilon = 0.05$ for frequency $f/4$ and $\epsilon = 0.08$ for frequency $f/2$. Note that $\frac{1}{\epsilon}$ is for both frequencies about a quarter of an acoustic wavelength (at $\theta = \pm 90°$).

It is more difficult to account for the shearing by the mean flow. Firstly, the model proposed by CH has no structure in the $x_2$ direction – the acoustic waves are assumed to be forced by the pressure at the centerline of the layer. The lateral dipole term $\sin\theta$ in (6) will surely be modified by the shear in a manner similar to the quadrupole components $A_{ij}$ discussed above. To ascertain the form of the directivity for a lateral dipole we solve Lilley's equation with a dipole source of the form

$$\Gamma = \bar{D}_t^2 \exp\left(2\pi i\omega t\right)\frac{\partial}{\partial x_2}\left(e^{-\pi(x_1/\epsilon_1)^2}e^{-\pi(x_2/\epsilon_2)^2}\right)/(\epsilon_1\epsilon_2), \tag{9}$$

where, as in (4), $\epsilon_1$ and $\epsilon_2$ control how compact the dipole is. The directivity for the dipole source in the mixing layer is now multiplied by the exponential term and the result plotted Figure 10, and the directivity produced by the total source $\Gamma$ is replotted also in Figure 10. The agreement, while still not quantitatively accurate, better accounts for the cusps and asymmetry of the computed directivity.

Finally, in Figure 11, we adjust the value of $\epsilon$ to fit the directivity of the sheared model with the directivity of the Lilley source – $\epsilon = 0.037$ is used for $f/2$ and $\epsilon = 0.051$ for $f/4$. Here the quantitative agreement is excellent. As we pointed out above, we believe that the difference between the full source and the Lilley source is attributable to scattering by the vortices and refraction effects due to the nonparallel mean flow. This leads us to further speculate that this is why the agreement with the superdirective model is so much better for the Lilley source than for the full source – one would not expect such a simplified model to take account of scattering or refraction by the nonparallel part of the mean flow.

## CONCLUSIONS

We have studied the sound generated by vortex pairing in a two-dimensional mixing layer using both DNS and a modified form of Lilley's acoustic analogy proposed by Goldstein (1984). The directivity of the acoustic far field at the pairing frequencies is highly directive and we have shown that it cannot be modeled by compact quadrupole sources, but is essentially of a superdirective nature, as in the model of Crighton and Huerre (1990). By making modifications to the their model we have accounted, in part, for shear in the mean velocity and the convection of the acoustic waves by the different freestream velocities on either side of the layer. With these modifications, the overall trends of the directivity compares very favorably with our numerical computations. Finally, the source term from the computations was decomposed into three contributions, one of which is the original source term proposed by Lilley leads to a more directive acoustic field than the full source, and which is in excellent quantitative agreement with our modified superdirective model (after constants have been adjusted). The other two terms appear to account mainly for scattering and refraction of the generated acoustic field and lead to smaller scale oscillations in the directivity which are not accounted for in the superdirective model.

## ACKNOWLEDGEMENTS

This work has been sponsored by the Office of Naval Research, grant N00014-92-J-1626, and computer time and support has been provided by the NASA Ames Research Center and the Center for Turbulence Research.

## REFERENCES


Colonius, T., Lele, S.K. and Moin, P., 1995, "The Sound Generated by a Two-Dimensional Shear Layer: A Comparison of Direct Computations and Acoustic Analogies," *CEAS/AIAA Paper 95-036.*

Colonius, T., Lele, S.K. and Moin, P., 1994a, "The scattering of sound waves by a vortex — numerical simulations and analytical solutions," *J. Fluid Mech.*, Vol. 260, pp. 271–298.

Colonius, T., 1994b, 'Direct Computation of Aerodynamic Sound' Ph.D. Thesis, Department of Mechanical Engineering, Stanford University.

Colonius, T., Lele, S.K., and Moin, P., 1993a, "Boundary conditions for direct computation of aerodynamic sound generation," *AIAA J.*, Vol. 31, pp. 1574–1582.

Crighton, D.G. and Huerre, P., 1990, "Shear-layer pressure fluctuations and superdirective acoustic sources," *J. Fluid Mech*, Vol. 220, pp. 355–368.

Goldstein, M.E., 1984, "Aeroacoustics of turbulent shear flows," *Ann. Rev. Fluid Mech.*, Vol. 16, pp. 263–285.

Goldstein, M.E., 1976, "The low frequency sound from multipole sources in axisymmetric shear flows. Part 2," *J. Fluid Mech.*, Vol. 75, pp. 17–28.

Goldstein, M.E., 1975, "The low frequency sound from multipole sources in axisymmetric shear flows, with application to jet noise," *J. Fluid Mech.*, Vol. 70, pp. 595–604.

Laufer, J. and Yen, T., 1983, "Noise generation by a low-Mach-number jet," *J. Fluid Mech.*, Vol. 134, pp. 1–31.

Lilley, G.M., 1974, 'On the noise from jets', *AGARD CP-131.* 345 pp.

Mitchell, B.E., Lele, S.K. and Moin, P., 1995a, "Direct Computation of the Sound Generated by Vortex Pairing in an Axisymmetric Jet," *AIAA Paper 95-0504.*

Mitchell, B.E., Lele, S.K. and Moin, P., 1995b, "Direct computation of the sound from a compressible co-rotating vortex pair," *J. Fluid Mech.*, Vol. 285, pp. 181–202.


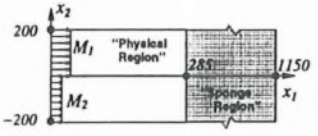


**Figure 1.** Schematic diagram of computational domain.

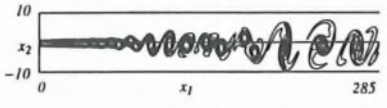


**Figure 2.** Vorticity contours in near field region. Contour levels: Min: -0.13, Max: 0.01, Increment: 0.02.

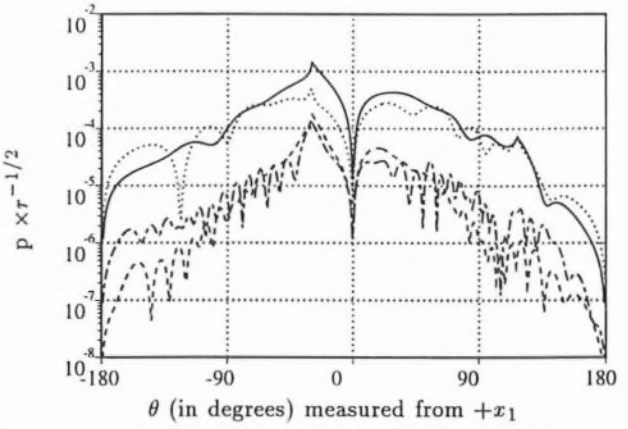


**Figure 3.** The asymptotic far field directivity resulting from: ——— The Lilley source at $f/4$; ····· The full source, $\Gamma$, at $f/4$; ---- The Lilley source at $f/2$; —·— The full source, $\Gamma$, at $f/2$.

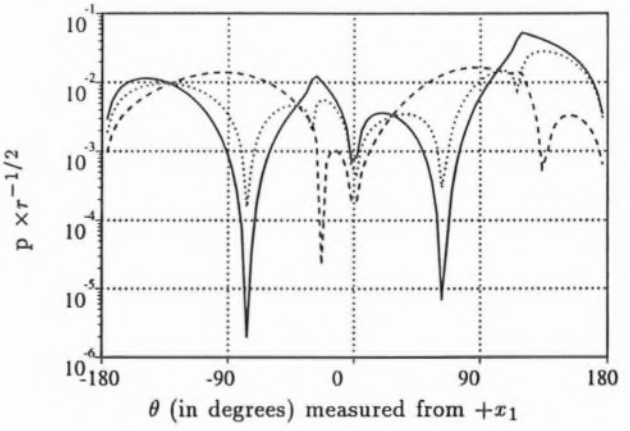


**Figure 4.** The far field directivity of stationary point quardrupole sources in a mixing layer at frequency $f/2$: ——— $A_{11}$ component only; ····· $A_{12}$ component only; ---- $A_{22}$ component only.

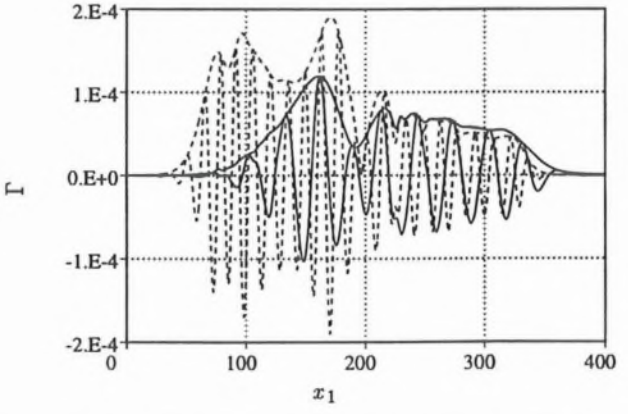


**Figure 5.** The DFT of $\Gamma$ at $x_2 = 0$ for $f/2$ and $f/4$. The real part and magnitude are shown–the imaginary part is similar to the real part in each case but shifted in phase by $\pi/2$. ——— $f/4$, ---- $f/2$.

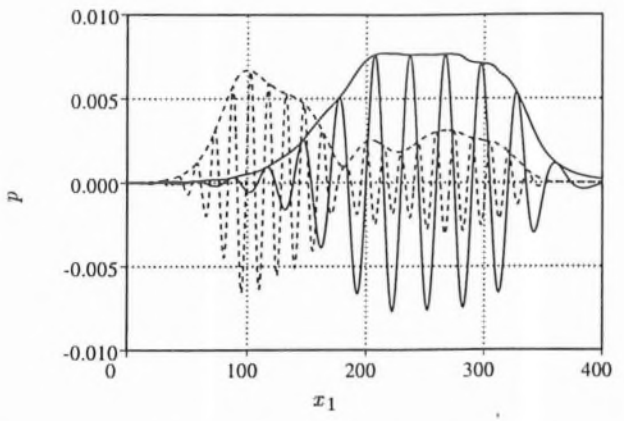


**Figure 6.** The DFT of $p$ at $x_2 = 0$ for $f/2$ and $f/4$. The real part and magnitude are shown–the imaginary part is similar to the real part in each case but shifted in phase by $\pi/2$. ——— $f/4$, ---- $f/2$.

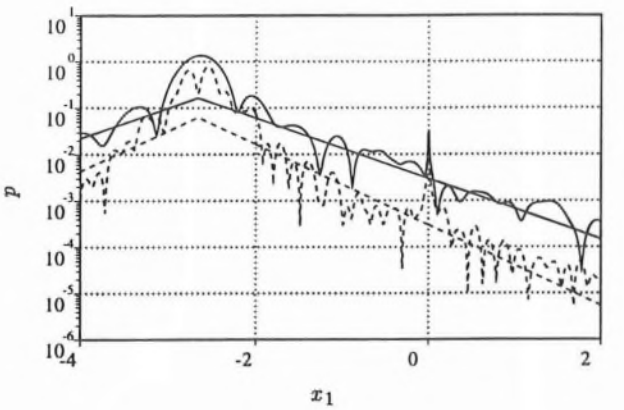


**Figure 7.** The magnitude of the Fourier transform in $x_1$ of the DFT of $p$ at $x_2 = 0$ for $f/2$ and $f/4$. The straight lines correspond to Equation (7): ——— $f/4$ ($\epsilon = 0.05$); ---- $f/2$ ($\epsilon = 0.08$).

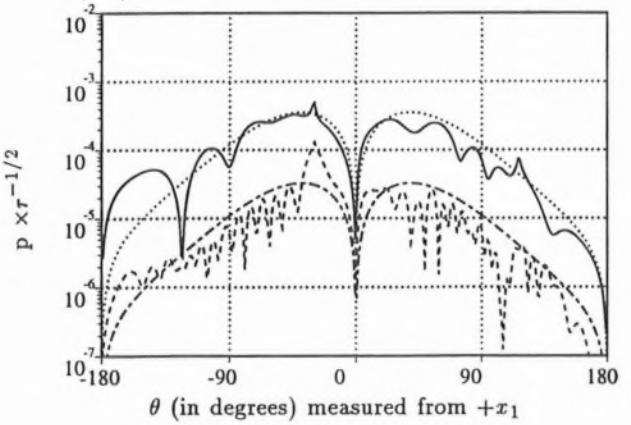


**Figure 8.** The asymptotic far field directivity resulting from: ——— The full source, $\Gamma$, at $f/4$; ····· Equation (6) with $a = 3.1$; ---- The full source, $\Gamma$, at $f/2$; —·— Equation (6) with $a = 5.0$.

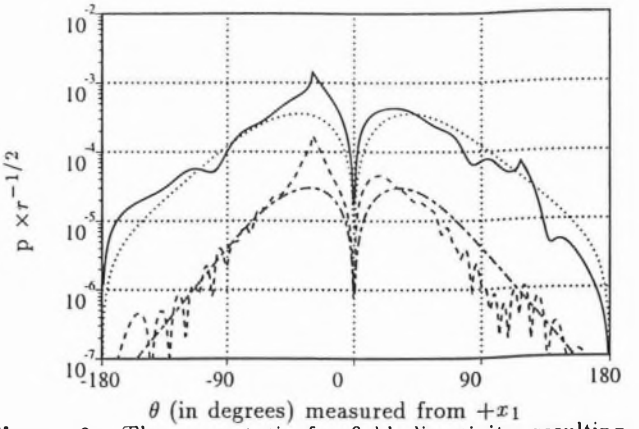


**Figure 9.** The asymptotic far field directivity resulting from: ——— The Lilley source at $f/4$; ····· Equation (6) with $a = 5.0$; ---- The Lilley source at $f/2$; —·— Equation (6) with $a = 8.5$.

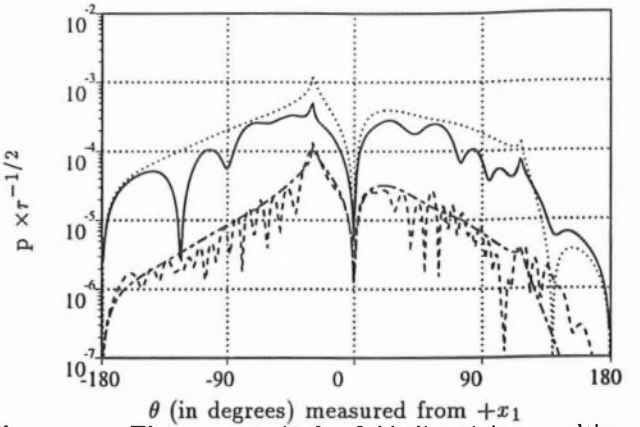


**Figure 10.** The asymptotic far field directivity resulting from: ——— The full source, $\Gamma$, at $f/4$; ····· Modified directivity (see text) at $f/4$; ---- The full source, $\Gamma$, at $f/2$; —·— Modified directivity (see text) at $f/2$.

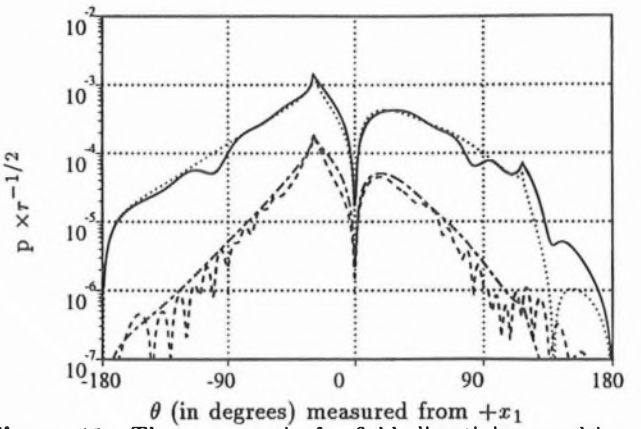


**Figure 11.** The asymptotic far field directivity resulting from: ——— The Lilley source at $f/4$; ····· Modified directivity (see text) at $f/4$; ---- The Lilley source at $f/2$; —·— Modified directivity (see text) at $f/2$.